



Transport of cohesive sediments.
Classification and requirements for turbulence
modelling.

A.W. Bruens
report no. 2-99

1999

Prepared for the European Commission, DG XII MAST3 - COSINUS Project, Con-
tract No. MAS3-CT97-0082



Hydromechanics Section, Faculty of Civil Engineering and Geosciences, Delft University of
Technology, P.O. Box 5048, 2600 GA, the Netherlands. Tel. +31 15 278 4070; Fax +31 15
278 59 75; E-mail: a.bruens@ct.tudelft.nl

Preface

The study described in this report is carried out in the framework of the MAST3-COSINUS Project (prediction of Cohesive sediment transport and bed dynamics in estuaries and coastal zones with Integrated Numerical simulation models). This COSINUS Project was initiated by several European research institutes and is funded in part by The European Commission, Directorate General XII for Science, Research & Development. The aim of this research project is to enhance the understanding of the behaviour of concentrated near-bed suspensions of cohesive sediments and their interaction with the water column and the sediment bed. This report describes progress made at Delft University of Technology on task A: Turbulence modelling of sediment-laden flow.

The work described in this report is part of a Ph.D project carried out at Delft University of Technology on the subject of cohesive sediment-laden flow.

Abstract

This report describes a classification of sediment-laden flows, which gives an overview of the different transport forms of fine sediment and the interactions of the different processes as acting in an estuary. At the outset of the proposed classification a distinction in physical states of water-sediment mixtures is made. A water-sediment mixture can exist in four physical states: 1) dilute suspension, in which the mutual interference between sediment particles and the turbulent flow field is negligible, 2) concentrated benthic suspension, in which sediment induced stratification and buoyancy become important, 3) fluid mud, in which the flocs start to form a network (a gel), the motion of fluid mud is laminar by definition, 4) consolidating bed, in which a strength, large enough to withstand the driving forces, has developed. The dynamics of a water-sediment mixture due to (hydrodynamic) forcing depend upon the different physical states in the vertical. On the other hand, the dynamical response of the mixture affects this vertical structure due to exchange processes at the interfaces between the different classes. The acting processes can be: (hindered) settling, deposition, entrainment, erosion, consolidation and liquefaction.

One of the objectives of the MAST3-COSINUS Project is to extend existing turbulence models in order to simulate sediment-laden flows for a wide range of Reynolds numbers. The molecular viscosity of sediment-water mixtures can be substantially larger than the viscosity of clear water. Due to buoyancy effects near interfaces or a decrease in driving forces, the turbulent viscosity can be substantially decreased, resulting in low Reynolds numbers. If the standard turbulence models do not predict these viscous effects, a low-Reynolds number turbulence model has to be implemented.

The 1DV POINT MODEL of Delft Hydraulics, with a constant molecular viscosity, is used for simulating the entrainment of a high-concentrated near bed layer. The agreement between experimental results and simulations is reasonable. Next a molecular viscosity depending on sediment concentration is implemented in the mean flow equation of the model. Preliminary results from this extended model show that in this model the fluid mud is dragged along by the overlying flowing fluid as is observed in experiments.

Contents

1	Introduction	2
2	Classification	4
2.1	Introduction	4
2.2	Physical states	5
2.3	Processes	8
2.3.1	Definitions	9
2.3.2	Processes in an estuarine environment	10
2.4	Vertical exchange processes	12
3	Requirements for turbulence modelling	16
3.1	Introduction	16
3.2	Requirements	16
3.3	Additional viscous effects	17
3.3.1	Viscous sublayer	18
3.3.2	(Reverse) transition	19
4	Example: simulating the resuspension of a concentrated layer	21
4.1	Introduction	21
4.2	The 1DV POINT MODEL	22
4.3	Testcases	23
4.4	The simulations	24
5	Future work	27
5.1	Introduction	27
5.2	Modelling laminarisation	27
5.3	Annular flume experiments	28
6	Acknowledgement	29
	References	30
	List of Figures	33

Chapter 1

Introduction

Fine-grained cohesive sediment is transported from fluvial and marine sources to depositional environments. The deposition of cohesive sediments can lead to a range of managerial problems. Examples of problem fields are maintenance of navigation channels, dredging and effects of construction works. To deal with these problems, it is essential to understand the behaviour of cohesive sediment and its interaction with the flow field. Settling from suspension alone cannot account for the often very high siltation rates. Hence it is expected that transport of sediment in high-concentrated layers near the bed is important.

In an estuary, many different processes are acting next to each other. Particles of cohesive sediment flocculate, the flocs can settle resulting in deposition. High-concentrated near bed layers can be formed, in which the flow can be either turbulent or laminar. Entrainment or erosion can occur at the interfaces of these layers. Under quiet conditions a high-concentrated near bed layer will consolidate. Figure 1.1 shows an example of a cross section of a part of an estuary showing these processes. The different kinds of physical processes affect each other. The net transport of mud is the result of the interaction of all the processes. As can be seen from figure 1.1, sediment-laden flow can pass from high into low Reynolds number flow and even into laminar flow, where the rheological properties of the material become dominant.

In the literature the various physical processes and the different flow conditions of sediment-laden flow have mostly been studied separately. In a typical paper one of the processes is highlighted and studied in detail. Hardly any attention has been paid to an overview of the different transport forms of fine sediment and the interactions of the different processes as acting in an estuary. Since the research on cohesive sediments started, a lot of progress has been made on the knowledge of the individual processes. Therefore it is useful to create a classification of sediment-laden flows, in which all the processes as shown in figure 1.1 are linked together.

This report describes a classification of sediment-laden flows, with emphasis on the physical processes. The objective of this classification is to give an overview of the various types of cohesive sediment-laden flows and vertical exchange of sediment in estuarine environments. The characteristics, formation and dynamics of sediment-laden flow as well as the interrelation of the physical processes are discussed.

The work reported was done in the framework of task A, turbulence modelling of sediment-

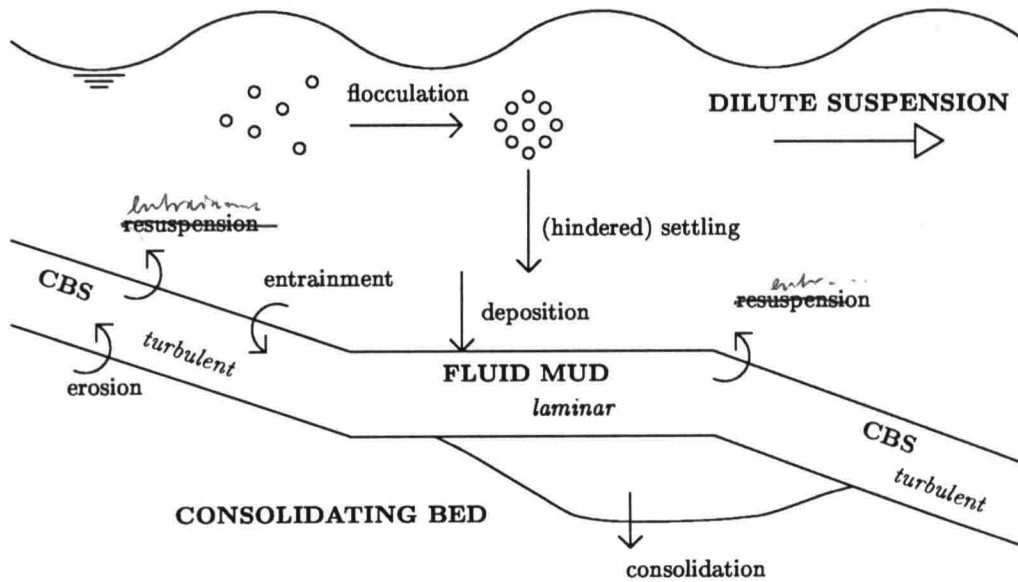


Figure 1.1: Example of a cross section of a part of an estuary.

laden flow, of the MAST3-COSINUS Project. One of the objectives of the COSINUS Project is to extend existing turbulence models in order to simulate sediment-laden flows for a wide range of Reynolds numbers. An overview on when we need a low-Reynolds-number turbulence model is still lacking. A starting point for judging the necessity of low-Reynolds-number modelling may be the following: if the standard turbulence models do not predict viscous effects which are actually significant, a low-Reynolds-number turbulence model will be needed (Kranenburg, 1998). Within the classification described in this report, an overview of flows is given for which additional viscous effects are physically relevant and a low-Reynolds-number model would be needed.

Outline

In chapter 2 the proposed classification of sediment-laden flow is described. The physical states of sediment-laden flows are discussed, followed by a description of the physical processes in estuarine and coastal waters.

Chapter 3 is concerned with the requirements for turbulence modelling. This chapter includes a discussion on when additional viscous effects are relevant and should be taken into account in turbulence models.

Chapter 4 of this report describes the simulation of entrainment of a dense lower-layer fluid by a turbulent upper layer. The 1DV POINT MODEL (Uittenbogaard *et al.*, 1996) including the standard $k - \epsilon$ turbulence model is used. The objective of this simulation is to examine the capability of the model to simulate this entrainment process.

Chapter 5 describes the planned future work.

Chapter 2

Classification

2.1 Introduction

Due to the cohesion of fine sediment, collisions of particles may result in aggregation. From studies by Van Leussen (1994) and Stolzenbach & Elimelech (1994), Winterwerp (1999) concludes that collision due to Brownian motion and differential settling is negligible in estuaries and that collision of particles can be totally attributed to turbulent motions. For small shear stresses aggregation is the dominant process, though at higher shear stresses breakup of flocs becomes the dominant process. The maximal attainable floc size is to a large extent determined by the residence time of the flocs. If the residence time is not the limiting factor, the floc diameter first increases and then decreases with increasing shear stress. The amount of collisions, and therefore the floc diameter, increases with sediment concentration. As a result of flocculation the floc diameter becomes the relevant parameter, instead of the particle diameter. The effective fall velocity of sediment depends on the floc diameter, and therefore on the aggregation and breakup of flocs.

Due to the gravitational force acting on the sediment flocs and counteracting the turbulent mixing, the sediment is prevented from uniformly mixing throughout the water column. At sufficiently high concentrations or sufficiently low turbulence levels, sediment falls out of suspension and the concentration increases towards the bed. Local regions of high gradients in the concentration can exist, so that a vertical concentration structure is developed.

Due to the presence of sediment particles, the physical state of a water-sediment mixture may differ from that of clear water. An increasing sediment concentration leads to a changing physical state. Therefore a vertical concentration structure leads to different physical states in the vertical. The concentrations at which transitions in physical states occur do not only depend on the characteristics of sediment and water, but also on external conditions (e.g. flocculation, flow conditions, stress history or time elapsed since deposition).

The dynamics of a water-sediment mixture due to (hydrodynamic) forcing depend upon this vertical structure. On the other hand, the dynamical response of the mixture affects the vertical structure. The prediction of mass transport is strongly contingent upon the understanding of this feedback mechanism between the vertical structure of the fine sediment and the flow field. In addition to this buoyancy effect, salinity may cause density stratification.

However, salinity-induced stratification is not considered herein.

At the outset of a classification of cohesive sediment-laden flows a distinction in physical states of water-sediment mixtures must be made. The next section defines the four physical states in which a water-sediment mixture can exist. The characteristic properties and the flow behaviour of the different classes are discussed. Section 2.2 describes the processes that interrelate the classes and deals with the formation of the classes under estuarine conditions. Section 2.3 deals with the vertical exchange of mass between the classes due to the dynamics of the water-sediment mixtures.

In literature different classifications of sediment-water mixtures can be found (Teeter, 1986; Mehta *et al.*, 1989; Winterwerp, 1996). Most of them are partial classifications and used to indicate the characteristics, concentrations etc. of the suspensions the author(s) examine(s). These classifications were not meant to give an overall overview of cohesive sediment transport.

2.2 Physical states

Vertical structure

Figure 2.1 shows a cross section of a water column in an estuary. The four classes of a water-sediment mixtures are indicated. Although all four classes are shown, this does not mean that all four classes are present throughout the whole tidal cycle or under all flow conditions (see section 2.3). Also, the interfaces between the different classes are indicated as sharp, but in reality the transitions between classes are gradual. The characteristic properties, the flow conditions and the dimensionless groups which characterise the four classes are listed in figure 2.1, and are discussed in the sequel of this section.

	Class	Flow conditions	Dominant dimensionless group
\bar{z}	1 Dilute suspension	turbulent	β
	2 CBS	turbulent	Ri_g
	3 Fluid mud	laminar	Re^e
	4 Consolidating bed	no flow (except creep)	τ_y/τ

Figure 2.1: The four physical states of a sediment-water mixture.

Dilute suspension (layer 1)

For very low sediment concentrations the characteristics of the water-sediment mixture are not substantially altered from that of clear water and the mutual interference between sediment particles and the turbulent flow field is negligible. Only minor vertical gradients in sediment concentration are present and in most cases buoyancy effects can be neglected. The viscosity is of the order of 10^{-6} m²/s, comparable to the viscosity of clear water, generally leading to large Reynolds numbers and turbulent flow conditions (even for small driving forces). The sediment particles and flocs are supported by turbulence induced forces and transported with the currents.

A water-sediment mixture having these characteristics is classified as a dilute suspension. Stratification induced by sediment generally does not occur in a dilute suspension and the parameter characterising this class is the dimensionless Rouse parameter, $\beta \propto w_s/u_*$, where w_s is the settling velocity of the sediment and u_* is the shear velocity. For β tending to zero, the concentration profile becomes uniform. A second criterion for a dilute suspension is a small gradient Richardson number, $Ri_g = -g \frac{\partial \rho}{\partial z} / \rho \left(\frac{\partial u}{\partial z} \right)^2$ where g is the accelerating force, ρ is the density, u is the horizontal velocity and z is the vertical coordinate (positive upwards), so that buoyancy is negligible. Different authors mention different maximum concentrations for a dilute suspension. The maximum concentration depends on flow velocity and fall velocity, it increases with increasing flow velocity and decreases with increasing fall velocity. According to Teeter (1986) concentrations have to be lower than 1 g/l while according to Ross (1988) the concentration should not exceed 0.5 g/l.

Concentrated benthic suspension (layer 2)

At higher sediment concentrations areas of large vertical gradients in sediment concentration develop, leading to density stratification. Buoyancy becomes important and turbulence is partially damped in these regions of high concentration gradients. This type of water-sediment mixture is classified as a concentrated benthic suspension, henceforth abbreviated as a CBS. The molecular viscosity of a CBS is still of the order 10^{-6} m²/s, generally leading to turbulent flow conditions.

At sediment concentrations exceeding approximately a few 10 g/l, the settling velocity of individual flocs decrease due to the influence of neighbouring flocs. This process is called hindered settling (see also section 2.3.1).

For low sediment concentrations the suspension behaves as a Newtonian fluid, i.e. the viscosity is constant by definition. For higher sediment concentrations though, the rheological properties change to non-Newtonian. The viscosity for non-Newtonian fluids depends on the shear rate, i.e. the relationship between shear-stress and shear rate is non-linear due to shear thinning. Also the stress response no longer solely depends on the deformation rate, but also on the deformation history. This phenomenon of time-dependent changes of the viscosity under constant shear is known as thixotropy.

Different authors mention different concentrations at which the transition to non-Newtonian behaviour occurs. Van Rijn (1993) and Krone (1986), among others, suggest that transition takes place at $c \approx 10$ g/l. A CBS is characterised by a large gradient Richardson number for

which buoyancy is relevant.

Fluid mud (layer 3)

For higher sediment concentrations the number of interfloc contacts increases and the flocs become space-filling. If the concentration reaches the gelling point c_g , the flocs start to form a network, called a gel, and the volume concentration of flocs in the water column, $\phi = c/c_g$, becomes equal to one. The rheological properties of fluid mud are non-Newtonian. The motion of fluid mud due to (hydrodynamic) forcing is laminar by definition.

For sediment concentrations exceeding the gelling point ($c > c_g$) hindered settling no longer occurs and further compaction is due to self-weight. At the onset of gelling, the excess weight of sediment is carried to a large extent by the pore water. If the formed fluid mud is not rapidly eroded, the excess pore water pressure (Δp) will gradually decrease, resulting in an increase in effective stress (σ' which is the difference between total stress and pore water pressure) and an increase in ϕ ($\phi > 1$). Despite the laminar motion this consolidation process may continue, although probably at a slower rate than for non-moving material.

Non-Newtonian material may be able to withstand stresses (i.e. no deformation occurs) below a certain yield stress (τ_y). The yield stress represents the particle interaction forces, by some authors indicated as the 'true cohesion', which has to be overcome to induce deformation. For sediment concentrations lower than 100 g/l, the yield stress usually is very small, $\tau_y \ll 0.1 \text{ N/m}^2$ (Van Rijn, 1993; Verreet & Berlamont, 1988). If the time scale for deposition is long enough, a measurable strength builds up. For sediment concentrations over 100 g/l, for example, the yield stress rapidly increases with concentration (Van Rijn, 1993; Verreet & Berlamont, 1988).

The concentration at which gelling starts depends on the floc diameter and therefore on the flocculation process, values reported in the literature lie between 50 g/l and 180 g/l (Winterwerp, 1999). The development of non-zero effective stresses also cannot be related to a precise density value, because it depends on the stress state and history of the deposit (Sills & Elder, 1986). From experiments in settling columns, Sills & Elder (1986) conclude that an effective stress can start to develop in the concentration range from 115 g/l to 220 g/l.

Reverse transition (from turbulent to laminar flow conditions) can be characterised by a critical value of the Reynolds number of turbulence. The Reynolds number of turbulence (Re_t) is defined by Ivey and Imberger (1991) as:

$$Re_t = \frac{u'L}{\nu} = \frac{1}{\sigma_t} \frac{\nu_t}{\nu} \quad (2.1)$$

where u' is the turbulence intensity, L is the length scale of the energy containing eddies, ν is the molecular viscosity, ν_t is the turbulent viscosity and σ_t is the turbulent Prandtl-Schmidt number. Transition (from laminar to turbulent flow conditions) in non-Newtonian material can be indicated by a critical effective Reynolds number. The effective Reynolds number is given by (Liu & Mei, 1990):

$$1/Re^e = 1/Re^\mu + 1/Re^\tau \quad (2.2)$$

where Re^μ represents a viscous part and Re^τ a yield stress. Fluid mud is characterised by an effective Reynolds number smaller than the critical value for transition.

Consolidating bed (layer 4)

Winterwerp (1999) indicates the importance of the ratio of the time scale of strength build-up and the time scale of the driving forces (the tide). If the material has enough time to build-up a strength large enough to withstand the driving forces ($\tau_y > \tau$, where τ is the stress due to the driving forces), the bed material stays at rest. Consolidation will continue in this consolidating bed, i.e. the expulsion of pore water and the increase of effective stress. The bed material is not flowing, the only possible motion is creep, which contributes to the consolidation process.

The characteristic parameter for a consolidating bed is a non-dimensional yield stress larger than one, $\tau_y/\tau > 1$. Also an increasing non-dimensional effective stress, $\sigma'/\Delta p$, characterises a consolidating bed.

2.3 Processes

The importance of the interrelationships between the classes of water-sediment mixture and the exchange of sediment between these classes was already discussed in section 2.1. The diagram in figure 2.2 gives an overview of the physical processes responsible for these interrelationships. The diagram is divided into two parts. On the right-hand side the classical floc deposition and erosion processes are presented, as studied by Krone (1962) and Partheniades (1962). The approach of these authors does not deal with the formation of high-concentrated

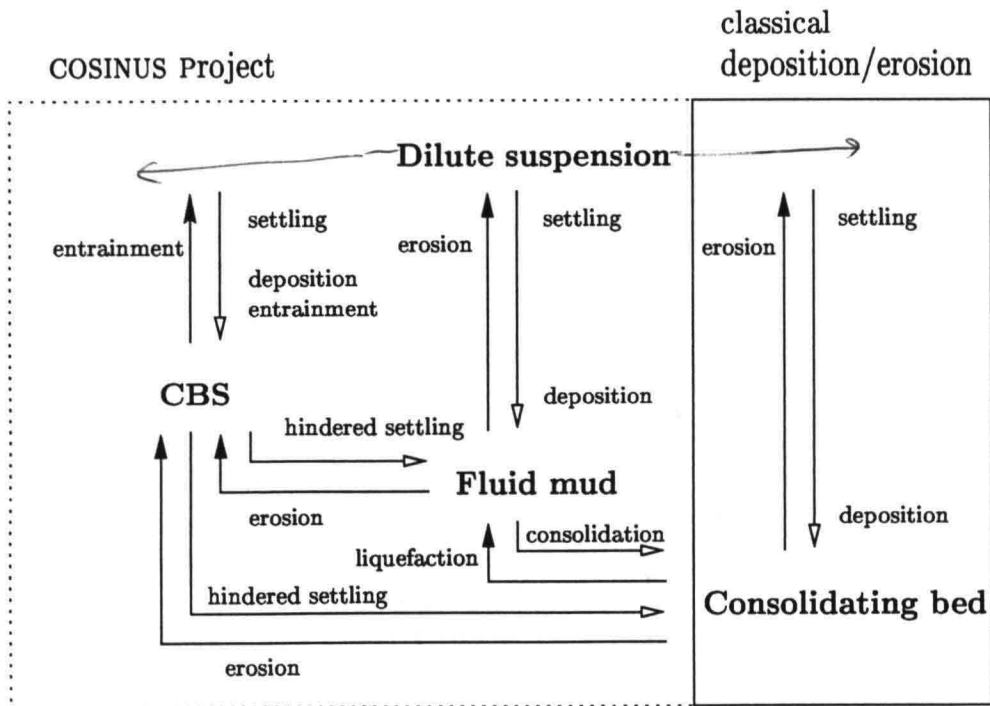


Figure 2.2: Diagram of the four classes and the physical exchange processes.

layers near the bed. On the left-hand side the relevant processes of the COSINUS Project are presented, that is, those related to CBS and fluid mud. As already mentioned in section 2.2, not all four classes of physical states have to be present. Figure 2.2 shows that CBS and/or fluid mud can be absent; the interactions between a CBS or a dilute suspension and a consolidating bed as well as interactions between a dilute suspension and a fluid mud are shown.

In section 2.3.1 the definitions of the processes indicated in figure 2.2 are given. Next the processes are described as acting in an estuarine environment, starting with the classical deposition and erosion processes followed by the COSINUS related processes.

2.3.1 Definitions

The following definitions are adopted herein.

Settling is the downward movement of sediment flocs due to gravitational forces and counteracted by viscous drag. The settling velocity depends on the floc diameter. In a turbulent flow settling is counteracted by turbulent diffusion, reducing the effective settling velocity.

Hindered settling is the decrease in settling velocity of an individual floc, due to the influence of neighbouring flocs at higher sediment concentrations ($c > 10$ g/l). The processes that lead to hindered settling (found in the literature and by physical reasoning) are summarised by Winterwerp (1999). Most important are return flow, the increase in effective viscosity of suspensions with high sediment concentrations and an increase of the bulk density of the surrounding fluid in which the flocs settle.

Deposition is the arrival of flocs at the layer below the layer in which settling occurred.

Entrainment is the inclusion of an ambient fluid by a fluid in turbulent motion. The ambient fluid is mixed into the turbulent fluid. The fluid entrained can be present on either side of a layer in which the flow is turbulent.

Erosion is the entrainment of material from a layer, in which a strength has developed. Two modes of erosion can be distinguished, bulk erosion and surface erosion. In the case of bulk erosion the turbulent shear stresses exceed the undrained strength of the material, failure may occur at some plane below the surface and a lump of material is eroded. Surface erosion is a drained erosion process. Which of the two erosion processes occurs in a particular case, depends on the ratio of undrained strength to the turbulent stresses (Van Kesteren, 1990).

Consolidation is the process of expulsion of pore water and the development of an effective stress and an increase in strength of the bed material under the influence of the excess self-weight of the consolidating material.

Liquefaction is the collapse of the grain matrix and the development of positive excess pore pressure. The flocs become fluid-supported and the effective stress decreases.

2.3.2 Processes in an estuarine environment

Classical floc deposition and erosion

If during slack water only a small amount of cohesive sediment is deposited on the consolidating bed, all the available sediment is easily entrained during the next tidal cycle. If a larger amount of sediment is deposited, a very strong current (e.g. during maximum tidal velocity) can still lead to the entrainment of all the available sediment. Under these conditions the available sediment is well mixed throughout the water column, leading to a low concentrated suspension from the bed up to the water surface. Only minor vertical concentration gradients then exist and the situation can be classified as a dilute suspension flowing over a consolidating bed.

Handwritten note: Dilute c.c.
✓

The rates of erosion and deposition of a consolidating bed by a dilute suspension are given by the classical floc erosion and deposition theory, as pointed out on the right hand side of figure 2.2. Krone (1962) showed that deposition is predominant when the bed-shear stress (τ_b) falls below a critical value for deposition (τ_d). Close to the bed the flocs are exposed to the largest shearing forces, due to the large velocity gradients in this region. Flocs with a low shear resistance are broken down in this region and resuspended. Flocs with a shear resistance high enough to withstand the shearing are deposited to the bed. Mehta & Partheniades (1975) found an equilibrium concentration (c_{eq}) after rapid deposition. This equilibrium concentration depends on the bed-shear stress, the type of sediment and the initial concentration (c_0). The ratio c_{eq}/c_0 represents the percentage of the flocs that remains in suspension, which implies that they have a shear strength lower than the bed-shear stress. Erosion of a consolidating bed occurs when the bed-shear stress exceeds a critical value for erosion (τ_e) (Partheniades, 1962). This critical value depends on the bed material characteristics and the bed structure.

Formation of a CBS and/or fluid mud

As a result of decreasing flow velocities, towards slack tide or due to a decreasing bed elevation (e.g. a navigation channel), the turbulent mixing will decrease and the sediment starts falling out of suspension. The upper part of the water column becomes clear first and a region of high concentration gradients (a downward moving lutocline) is formed, which influences the turbulent properties due to buoyancy. The sediment concentration increases towards the bed and a CBS is formed (indicated by the downward arrow between dilute suspension and CBS in figure 2.2). For the exchange between CBS and bed the classical erosion and deposition formulations (see previous section) are probably valid. In figure 2.2 these processes are indicated by the arrows for erosion and deposition between CBS and consolidating bed.

For concentrations exceeding 10 g/l the settling velocity decreases (because of hindered settling), leading to lower settling velocities near the bed than higher in the water column. The result is an increasing accumulation of sediment particles lower in the water column. As long as the settling rate in the upper part is larger than the deposition rate at the bottom the thickness of this high-concentrated near bed layer increases (that is a rising lutocline). If the amount of sediment in suspension (which is available for settling) is large and the time of accumulation is sufficiently long, the sediment concentration increases and the gelling point

can be reached ($c = c_g$), resulting in the transition from CBS into fluid mud (see downward arrow between CBS and fluid mud and between dilute suspension and fluid mud).

Due to the excess weight of sediment consolidation of the fluid mud continues, increasing the effective stress and the strength of the material. If the time scale of the driving forces (the tide) is large compared to the time scale of consolidation, i.e. if a strength can be build up before the material is eroded, transition towards a consolidating bed occurs on the lower part of the fluid mud (downward arrow between fluid mud and consolidating bed). The resulting configuration of the processes in this paragraph can be: (1) all four classes present, (2) a dilute suspension, a CBS and a consolidating bed, (3) a dilute suspension, fluid mud and a consolidating bed.

Another way of fluid mud formation is due to the sediment-induced collapse of turbulence at a critical flux Richardson number. This results in a flow which is no longer able to carry the sediment in suspension (Winterwerp, 1998). The turbulence collapses when the flux Richardson number exceeds a critical value of about 0.15. This critical value can be reached by an increasing sediment concentration (due to continues erosion of a consolidating bed) or by a sudden decrease in flow velocity.

Due to liquefaction of a consolidating bed, the mud becomes fluid and the flocs are supported again by the fluid. This is shown by the arrow between consolidating bed and fluid mud in figure 2.2.

Resuspension of CBS and/or erosion of fluid mud

Increasing flow velocities, towards maximum tidal velocities or due to wind forcing for example, can result in the entrainment of a CBS and/or the erosion of a fluid mud layer. First the configuration of a dilute suspension on top of fluid mud is considered. Pressure gradients due to tidal conditions result in the generation of turbulence at the interface between fluid mud and dilute suspension, resulting in a turbulent dilute suspension flowing over fluid mud. These dynamics are comparable with the dynamics due to wind forcing. Due to the turbulent motion, the dilute suspension starts to erode the top of the fluid mud layer (upward arrow between fluid mud and dilute suspension). If the eroded material is rapidly mixed throughout the water column, the lutocline moves downward to the bed. If the currents are sufficiently strong (for example during spring tides), the fluid mud is totally eroded. The result is the same configuration as at the beginning of this section: a dilute suspension flowing over a consolidating bed. For weaker currents (for example during neap tides) only part of the deposited fluid mud may be eroded and a vertical structure of a dilute suspension, fluid mud and a consolidating bed will remain.

For the configuration of a dilute suspension, a CBS, a possible fluid mud layer and a consolidating bed, different dynamic processes occur. The CBS layer will not be strong enough to resist the longitudinal pressure gradient due to tidal flow and a flow is induced in the CBS (Kranenburg & Bruens, 1998). Turbulence is generated at the interface between CBS and the consolidating bed (or at the CBS-fluid mud interface) due to bed friction (or friction at the CBS-fluid mud interface). The result is a turbulent CBS entraining the overlying dilute suspension (resulting in a rising lutocline) and eroding the consolidating bed (or fluid mud) below. These processes are indicated by the downward arrow between dilute suspension and

CBS and the upward arrow between fluid mud and CBS. This behaviour of a CBS has been observed in the field (Le Hir, 1997) and a laboratory experiment on this entrainment process is planned within task C of the COSINUS Project (Kranenburg & Bruens, 1998). When the CBS flow is sufficiently strong the sediment in the CBS and possibly the fluid mud are mixed throughout the water column. This again results in the configuration of a dilute suspension flowing over a consolidating bed. For weaker currents the configuration of dilute suspension, CBS (and fluid mud), and consolidating bed will remain.

Due to wind action on the free surface of a dilute suspension, turbulence is generated in the dilute suspension. The CBS layer can be entrained by this turbulent dilute suspension flowing over the CBS layer.

2.4 Vertical exchange processes

In this section the vertical exchange processes of fine-sediment at the interfaces between the various types of fine-sediment appearances are reviewed. The exchange processes result from the dynamics of the water-sediment mixtures. As argued in section 2.1: *The dynamics of a water-sediment mixture due to (hydrodynamic) forcing depend upon the vertical structure of sediment appearances. On the other hand, the dynamical response of the mixture affects this vertical structure.*

Two basically different configurations are discussed. Both configurations can be observed in estuarine environments and are already described in section 2.3.2. The first configuration consists of a turbulent CBS flowing under a dilute suspension, the second of a turbulent dilute suspension flowing over fluid mud. The vertical exchange processes differ for the two situations, leading to different interrelating arrows in figure 3.

Entrainment by a CBS layer

An example of a turbulent CBS under a dilute suspension is shown in figure 2.3. During low velocities (slack tide) a CBS and possibly a fluid mud is deposited. Pressure gradients due to tidal flow result thereupon in the generation of turbulence in the CBS. Figure 2.3a shows a schematic cross section of this configuration. At interface 1-2 the dilute suspension is entrained during high turbulent flow in the CBS. At the same time material from the dilute suspension can be deposited at this interface. At interface 2-3 the fluid mud may be eroded during high turbulent flow in the CBS, in that case the stress at this interface, τ_{2-3} , exceeds the critical stress for erosion ($\tau_{2-3} > \tau_e$). Material is deposited during low-level turbulence conditions in the CBS ($\tau_{2-3} < \tau_d$). At interface 3-4 consolidation results in the transition of fluid mud into a consolidating bed. Figure 2.3b indicates that as a result of the entrainment of dilute suspension, the bulk density of the CBS decreases while the lutocline rises. Figure 2.3c shows that as turbulence is generated in the CBS, the eddy viscosity in this layer can be much larger than in the dilute suspension (Winterwerp, 1999).

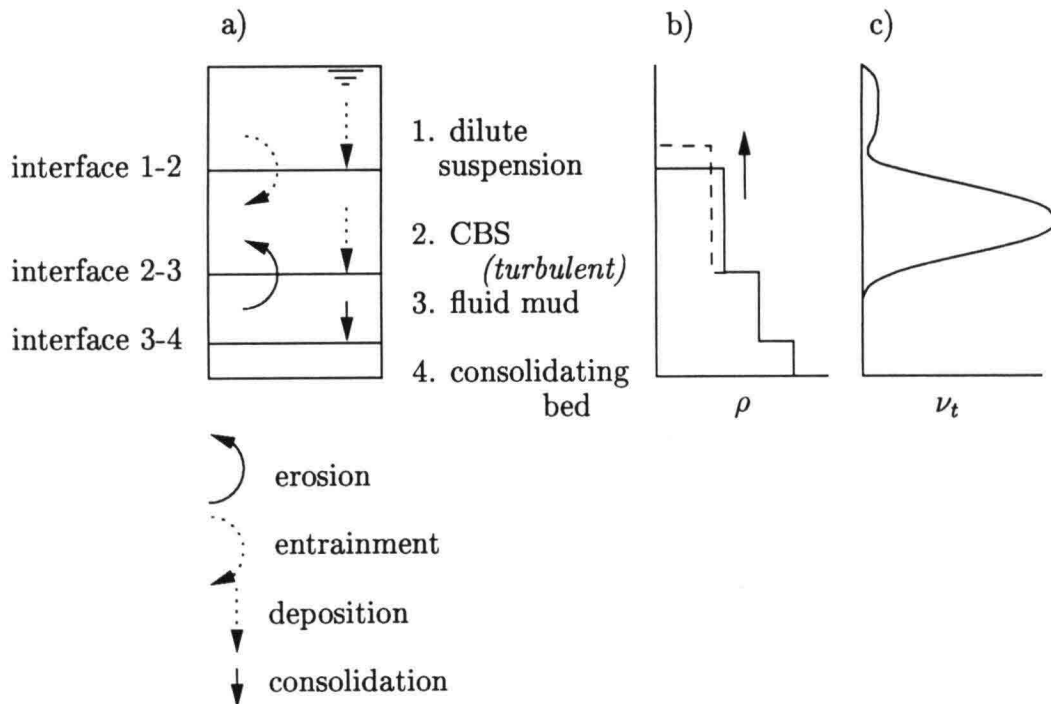


Figure 2.3: Processes acting in case of a turbulent CBS, (a) a schematic cross section, (b) the density profile showing a rising lutocline, (c) the eddy viscosity profile.

Entrainment by a dilute suspension

An example of a turbulent dilute suspension flowing over a fluid mud is shown in figure 2.4. During low flow velocities (slack tide) fine sediment has been deposited in, for example, a navigation channel and has formed fluid mud. On the onset of flood or ebb tide a turbulent dilute suspension starts flowing over this fluid mud. Figure 2.4a shows a schematic cross section of this configuration. At interface 1-3 material can be eroded from the fluid mud (strong currents, $\tau_{1-3} > \tau_e$) or material can be deposited (weak currents $\tau_{1-3} < \tau_d$). At interface 3-4 consolidation is the acting process. Due to the erosion of fluid mud, the density in the dilute suspension increases and the lutocline is moving towards the bed (figure 2.4b). Figure 2.4c shows the distribution of the eddy viscosity.

Figure 2.5 summarises the possible processes under tidal conditions at the various interfaces. The columns represent the processes, while the rows present the interfaces. In the cells the direction of transport of material is indicated by $x \rightarrow y$, meaning that mass (water, or sediment and water) from layer x is transported to layer y .

The $1 \rightarrow 2$ in the upper cell in the entrainment column represents the entrainment of a dilute suspension by a CBS, due to the generation of turbulence in the CBS at the onset

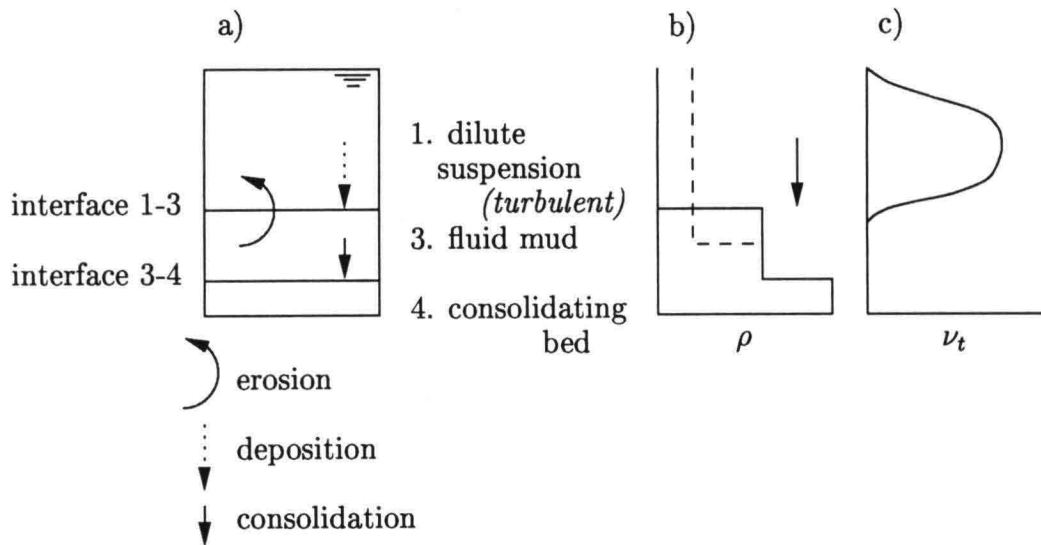


Figure 2.4: Processes acting in case of a turbulent dilute suspension, (a) schematic cross section, (b) the density profile showing a downward moving lutocline, (c) the eddy viscosity profile.

interface	entrainment	erosion	deposition	consolidation	liquefaction
1-2	$\begin{matrix} 1 \rightarrow 2 \\ 2 \rightarrow 1 \end{matrix}$		$1 \rightarrow 2$		
2-3		$3 \rightarrow 2$	$2 \rightarrow 3$		
1-3		$3 \rightarrow 1$	$1 \rightarrow 3$		
3-4				$3 \rightarrow 4$	$4 \rightarrow 3$
2-4		$4 \rightarrow 2$	$2 \rightarrow 4$		
1-4		$4 \rightarrow 1$	$1 \rightarrow 4$		

1 = dilute suspension
 2 = CBS
 3 = fluid mud
 4 = consolidating bed

Figure 2.5: Exchange processes.

of the tide. In that case, mass is transported from layer 1 (dilute suspension) to layer 2 (CBS). The $2 \rightarrow 1$ in the upper cell in this column represents the entrainment of CBS by a dilute suspension (due to wind forcing, for example). In the third column the erosion of fluid mud by a highly turbulent CBS or by a dilute suspension is indicated. The erosion of a consolidating bed by a dilute suspension or a CBS is also indicated in this column. Deposition can occur at all interfaces except the interface between fluid mud and consolidating bed at which consolidation occurs (fourth and fifth column). Liquefaction of a consolidating bed is indicated in the last column.

From laboratory experiments it appeared that erosion and deposition do not occur simultaneously ($\tau_e > \tau_d$). Though, it is argued that under field conditions the variability of the shear stress at the interfaces is considerable larger, allowing simultaneous erosion and deposition at different locations, or in succession at one particular location (Teisson, 1997).

All the arrows in table 1 correspond with an arrow in figure 3. The arrow in the upper cell in the first column, for example, corresponds with the downward arrow between dilute suspension and CBS in figure 3.

Chapter 3

Requirements for turbulence modelling

3.1 Introduction

Numerical models are widely used to predict the transport of cohesive sediments in estuarine environments. The performance of a numerical model depends on the implementation of the processes described in chapter 1. The first numerical models were developed in the 1970's, since then numerous transport models, from simple depth integrated and one-dimensional models to three-dimensional models for more complex situations, are developed. The knowledge of the individual processes as well as the computer capacities have increased during the last decades. Hopefully this progress is continued, so that in the near future numerical models meet the requirements for accurate prediction of cohesive sediment transport needed for safe navigation, solving water quality problems and disposal site problems.

The next section discusses briefly the requirements for sound turbulence modelling of the different types of fine-sediment appearances. Some of the requirements can be achieved with the present knowledge, other requirements still raise unsolved problems.

As stated earlier, an overview on when we need a low-Reynolds number turbulence model is still lacking. In section 3.3 an overview of flows is given for which additional viscous effects are physically relevant.

3.2 Requirements

The sediment related processes in a dilute suspension are aggregation of flocs, break up of flocs and settling of flocs. For sound modelling it is needed to model the flocculation, which is the combined process of aggregation and floc breakup, as well as the relation between settling velocity and floc size accurately. In estuarine and coastal environments, the flocculation process can be mainly contributed to turbulence. At small shear stresses the dominant process is aggregation, at larger shear stresses the break up of flocs becomes dominant. The dissipation parameter G , $G = (\epsilon/\nu)^{0.5} = \nu/\lambda_0^2$ where ϵ is the turbulent dissipation rate per unit mass and λ_0 is the Kolmogorov micro-scale of turbulence, is an important parameter for sound

flocculation modelling. Winterwerp (1999) derives a formula for the flocculation of cohesive sediment under the influence of turbulent shear. Teisson (1997) shows that the size and density of flocs are important for the generation of high-concentrated near-bed layers, as already mentioned by Krone (1986). Model results have shown that the volumetric concentration is a more relevant parameter controlling the processes than the mass concentration.

In a Newtonian CBS hindered settling and sediment induced stratification become important. For modelling hindered settling, an equation expressing the decrease in settling velocity at increasing (volumetric) sediment concentration have to be implemented. Density stratification leads to a reduction in eddy viscosity and eddy diffusivity. In Prandtl mixing-length turbulence models, for example, damping functions are used to model this stratification effect. In $k - \epsilon$ models, for example, this effect is accounted for by a buoyancy destruction term in the transport equation for the turbulent kinetic energy (see equation 4.3).

In stratified flows internal waves may generate turbulence (Uittenbogaard, 1995). It remains to be seen whether internal-wave effects have to be included in turbulence modelling for CBS flows.

The modelling of non-Newtonian fluid becomes more complicated as the molecular viscosity is no longer constant, but depends on the shear rate and on the shear history.

Consolidation results in an increasing yield strength, therefore influences the erosion rate and indirectly the turbulence modelling. For the erosion rate of a bed with constant density Partheniades (1962) found (for $\tau_b > \tau_e$):

$$E = M \left[\frac{\tau_b - \tau_e}{\tau_e} \right] \quad (3.1)$$

where M represents a material coefficient in mass per unit area and time. For a soft bed of increasing density (τ_e not constant) Parchure and Mehta (1985) found (for $\tau_b > \tau_e(z)$):

$$E = E_0 \exp \left[\alpha (\tau_b - \tau_e)^{0.5} \right] \quad (3.2)$$

Most models do not deal with the bed yield strength, but relate the critical stress for erosion to the density of the bed (ρ_b), e.g. by a power law:

$$\tau_e = a \rho_b^c \quad (3.3)$$

where a and c are empirical coefficients. In this case a consolidation model should reproduce the vertical density profile.

3.3 Additional viscous effects

The molecular viscosity of clear water is almost always small compared to the eddy viscosity so that the Reynolds number is large. Depending on the sediment concentration and the shear stress, the molecular viscosity of sediment-water mixtures can be substantially larger (De Wit, 1992). Due to buoyancy effects near interfaces or a decrease in driving forces, the turbulent viscosity can be substantially decreased. Therefore the presence of suspended particles or flocs can reduce the Reynolds number of turbulence. At sufficiently low Reynolds

numbers a transition from turbulent to laminar flow conditions can occur. In this section the configurations are discussed for which the molecular viscosity of the fluid becomes relatively large and viscous effects may be relevant. If the standard turbulence models do not predict these viscous effects, a low-Reynolds number turbulence model has to be implemented.

The Reynolds number of turbulence is reduced in areas where the turbulence is damped and the molecular viscosity becomes relatively large. This occurs near an interface, as large concentration gradients in these areas lead to damping of turbulence. The result, a viscous sublayer near the interface, is discussed in section 3.3.1.

The Reynolds number of turbulence can also be reduced in case of decreasing driving forces (e.g. a decreasing bed slope or decreasing pressure gradients towards slack tide). The sediment-laden flow can pass from high into low Reynolds number flow and eventually in laminar flow (see also figure 1.1). Vice versa, due to increasing driving forces (e.g. an increasing bed slope or towards maximum tide velocities) the flow can pass from laminar into low Reynolds and eventually high Reynolds number flow. Section 3.3.2 deals with these (reverse) transition processes.

3.3.1 Viscous sublayer

Figure 2.3 shows a cross-section of a water column including a dilute suspension-CBS interface and a CBS-fluid mud interface. The CBS in this example is highly turbulent (see section 2.4). Figure 2.3c shows the eddy viscosity profile. The eddy viscosity decreases towards the interfaces and almost goes to zero.

For the damping of turbulence in clear water near a solid wall, low-Reynolds number turbulence models have been developed. Most researchers, see Patel *et al.* (1985), propose multiplying the expression for the eddy viscosity in the $k - \epsilon$ model by a factor f_μ :

$$\nu_t = c_\mu f_\mu \frac{k^2}{\epsilon} \quad (3.4)$$

where f_μ is a function of a Reynolds number of turbulence, ν_t is the eddy viscosity, k is the turbulent kinetic energy, ϵ is the dissipation rate and c_μ is a coefficient. When the Reynolds number is high (away from the wall), the flow is fully turbulent and f_μ is equal to 1. For a decreasing Reynolds number (closer to the wall) f_μ decreases, and f_μ goes to zero for a vanishing Reynolds number (at the wall). In figure 3.3.1 (Patel *et al.*, 1985) f_μ is plotted against y^+ , the non-dimensionalised distance from the solid wall:

$$y^+ = \frac{u_* y}{\nu_m} \quad (3.5)$$

where u_* is the friction velocity, y is the distance from the wall and ν_m is the molecular kinematic viscosity. Viscous effects are important for y^+ less than about 50. In case of a very low-concentrated fluid with $\nu_m \approx 1 \cdot 10^{-6} \text{ m}^2/\text{s}$ and $u_* = 0.01 \text{ m/s}$, for example, viscous damping is of importance for $y < 5 \text{ mm}$. For high concentrated suspensions with for example $\nu_m \approx 1 \cdot 10^{-5} \text{ m}^2/\text{s}$ damping extends to the area $y < 5 \text{ cm}$. In addition, viscosity may enhance the damping of turbulence resulting from density stratification. However, damping caused by buoyancy is overestimated in the standard $k - \epsilon$ model and implementing a low-Reynolds

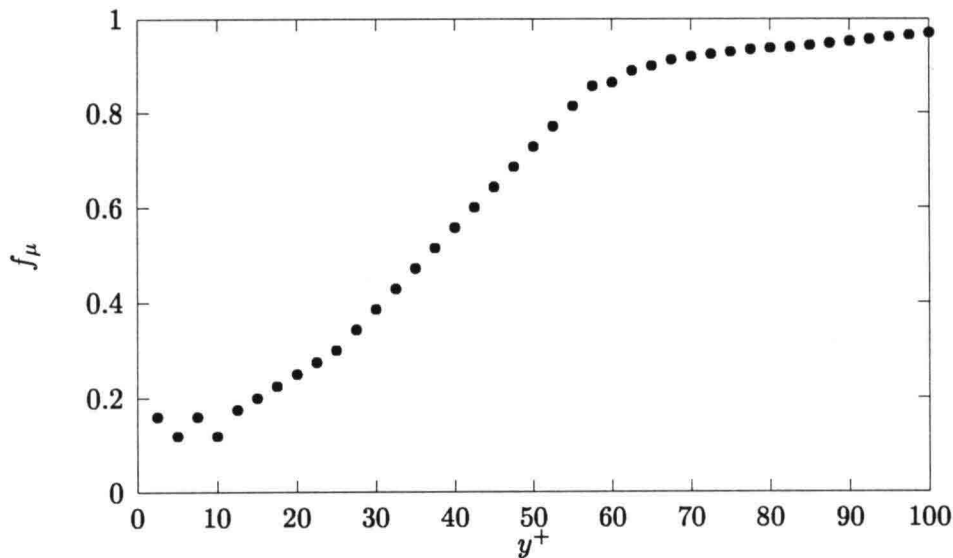


Figure 3.1: Variation of the function f_μ with distance from a smooth wall Patel *et al.*, 1985.

number model might deteriorate the results. Also, if over a large area the molecular viscosity stays substantially small compared to the eddy viscosity ($\nu_t \gg \nu_m$), a low Reynolds number is redundant. If near interfaces the turbulence is suppressed by buoyancy before viscous effects become important, a low-Reynolds number turbulence model is redundant.

3.3.2 (Reverse) transition

In figure 1.1 an example of both reverse transition and transition is shown. Due to a decrease or increase in slope, the near bed concentrated suspension can pass from CBS into fluid mud or from fluid mud into CBS respectively. The turbulent viscosity is reduced for decreasing driving forces and the flow can become laminar, this reverse transition occurs gradually. In the standard $k - \epsilon$ model, the Reynolds number at which this transition occurs is too low (Uittenbogaard, personal communication 1998). A low-Reynolds adaptation has to be implemented in order to simulate the physical process of reduction in turbulence level and the transition at the correct Reynolds number. In a Prandtl mixing-length model, including the Van Driest model of low-Reynolds-number flows, transition can only be modelled by explicitly imposing a critical value of the turbulence Reynolds number at which the flow becomes laminar (Kranenburg, 1999).

The critical value of the turbulence Reynolds numbers differs for transition and reverse transition. Also, transition occurs abruptly, while reverse transition occurs gradually. This implies that the adaptation for modelling transition differs from the adaptation for modelling reverse transition.

	interface	transition	reverse transition
dilute suspension	-	-	-
CBS	(+)	+ 	+ 
fluid mud	+	+ 	+ 
consolidating bed	-	-	-

+ = relevant
 - = not relevant

Figure 3.2: The relevance of additional viscous effects for the four different sediment classes.

Figure 3.2 indicates for which classes of sediment suspensions additional viscous effects are relevant. In a dilute suspension viscous effects are present near interfaces, but only over a very small area (< 5 mm see section 3.3.1). Hence they can be neglected and are indicated as not relevant in figure 3.2. In a CBS the viscous effects near interfaces may be relevant if the turbulence is not suppressed by stratification. In a fluid mud viscous effects are relevant as the molecular viscosity is high and the flow is laminar. Flow in a dilute suspension is almost always turbulent and (reverse) transition is not relevant. Due to (reverse) transition the sediment-water mixture can change from CBS into fluid mud or vice versa, this is indicated by the arrows in figure 3.2.

Chapter 4

Example: simulating the resuspension of a concentrated layer

4.1 Introduction

Mathematical models are widely used as tools for solving managerial problems in estuarine and coastal environments. Examples of application fields are maintenance of navigation channels, dredging and effects of construction works. To deal with most of these problems not only the water movement has to be modelled, but also the sediment transport. At present the behaviour of concentrated near-bed suspensions cannot be modelled accurately enough, owing to a lack of understanding of the physical processes in these suspensions.

The transport of sediment is partly governed by the entrainment process of freshly deposited high concentrated near-bed layers (see section 2.3 and 2.4). In this study the entrainment of a dense lower-layer fluid is simulated, using the 1DV POINT MODEL (Uittenbogaard *et al.*, 1996) including a $k - \epsilon$ turbulence model. The influence of viscosity of fluid mud, which can be quite large, on mean flow conditions and turbulence is not yet taken into account in the 1DV POINT MODEL. From measurements by De Wit (1992) and Wan (1982) the following empirical correlation between viscosity and sediment concentration was derived by Van Kessel (1997) :

$$\mu_m = \mu_w(1 + aN^b) \quad (4.1)$$

where μ_m is the molecular dynamic viscosity, μ_w is the molecular dynamic viscosity of water, N is the volumetric concentration and a and b are coefficients. For De Wit's measurements at a shear rate of 50 s^{-1} these coefficients are 933 and 1.98 respectively. For shear rates of approximately 1 s^{-1} a can become 10 times larger ($a \approx 9330$). The objective of this study is to indicate whether viscosity is essential to dependable modelling of sediment-laden flow.

The following methodology is applied: first entrainment of a dense lower-layer fluid is simulated with the standard model, in order to examine the accuracy of this model. Next a molecular viscosity depending on sediment concentration (equation 4.1) is implemented in the mean flow equation of the model and the entrainment of a dense layer is again simulated. The results show whether this extended model is capable of sound modelling.

A description of the 1DV POINT MODEL is given in the next section. Section 4.3 describes the testcases and the results of the simulations are presented in section 4.4.

4.2 The 1DV POINT MODEL

This section gives a summary of the equations in the 1DV POINT MODEL. Detailed descriptions are presented by Uittenbogaard *et al.* (1996) and Winterwerp and Uittenbogaard (1997).

The model treats the sediment-water mixture as a single-phase fluid in which all the particles follow the turbulence movements, but for their settling velocity. All horizontal velocity and concentration gradients are neglected and the horizontal velocity (u) is in one direction only. The momentum equation then reads:

$$\frac{\partial u}{\partial t} + \frac{1}{\rho} \frac{\partial p}{\partial x} = \frac{\partial}{\partial z} \left\{ (\nu + \nu_t) \frac{\partial u}{\partial z} \right\} \quad (4.2)$$

where p is pressure, t is time, x is the horizontal coordinate, z is the vertical coordinate, ρ is the bulk density of the mixture, ν is the molecular viscosity, and ν_t is the turbulent viscosity. The turbulent transport terms are modelled as a diffusion process:

$$\overline{u'w'} = -\nu_t \frac{\partial u}{\partial z}; \quad \overline{\rho'w'} = -\Gamma_t \frac{\partial \rho}{\partial z}$$

in which a prime denotes turbulent fluctuations and an overbar ensemble averaging over the turbulent time scale, w represents the vertical velocity and Γ_t represents the eddy diffusivity.

A $k - \epsilon$ model that consist of a transport equation for the turbulent kinetic energy (k) and the turbulent dissipation (ϵ) is implemented in the 1DV POINT MODEL:

$$\frac{\partial k}{\partial t} = \frac{\partial}{\partial z} \left\{ (\nu + \Gamma_t^{(k)}) \frac{\partial k}{\partial z} \right\} + \nu_t \left(\frac{\partial u}{\partial z} \right)^2 - \Gamma_t \frac{g}{\rho} \frac{\partial \rho}{\partial z} - \epsilon \quad (4.3)$$

$$\frac{\partial \epsilon}{\partial t} = \frac{\partial}{\partial z} \left\{ (\nu + \Gamma_t^{(\epsilon)}) \frac{\partial \epsilon}{\partial z} \right\} + c_{1\epsilon} \frac{\epsilon}{k} \nu_t \left(\frac{\partial u}{\partial z} \right)^2 - c_{1\epsilon} (1 - c_{3\epsilon}) \frac{\epsilon}{k} \Gamma_t \frac{g}{\rho} \frac{\partial \rho}{\partial z} - c_{2\epsilon} \frac{\epsilon^2}{k} \quad (4.4)$$

The eddy viscosity (ν_t) and eddy diffusivity (Γ_t) are given by:

$$\nu_t = c_\mu \frac{k^2}{\epsilon}; \quad \Gamma_t^{(i)} = \frac{\nu_t}{\sigma_t^{(i)}}$$

in which $\sigma_t^{(i)}$ is the Prandtl Schmidt number. The constants in the $k - \epsilon$ model have been found from calibration against laboratory data of grid-generated turbulence and boundary layer flow:

$$\begin{aligned} c_\mu &= 0.09; & c_{1\epsilon} &= 1.44; & c_{2\epsilon} &= 1.92; & \sigma_t^{(k)} &= 1.0; \\ \sigma_t^{(\epsilon)} &= 1.3; & \sigma_t^{(\rho)} &= 0.7 & \kappa &= 0.41; \\ c_{3\epsilon} &= 1 & \text{for} & & \frac{\partial \rho}{\partial z} &\leq 0; \\ c_{3\epsilon} &= 0 & \text{for} & & \frac{\partial \rho}{\partial z} &> 0 \end{aligned}$$

The bulk density is not only a function of salinity and temperature but also of the suspended sediment concentration according to:

$$\rho(s, \theta, c^{(l)}) = \rho_w(s, \theta) + \sum_l \left(1 - \frac{\rho_w(s, \theta)}{\rho_s^{(l)}} \right) c^{(l)} \quad (4.5)$$

where s is salinity, θ is temperature, ρ_w is the density of water, $c^{(l)}$ is the suspended sediment concentration by mass of fraction l and $\rho_s^{(l)}$ is the specific density of fraction l .

The equation for mass concentration $c^{(l)}$ of any sediment of fraction l reads:

$$\frac{\partial c^{(l)}}{\partial t} - \frac{\partial w_s^{(l)} c^{(l)}}{\partial z} = \frac{\partial \phi}{\partial z} \left\{ (D_c^{(l)}) + \Gamma_t^{(l)} \right\} \frac{\partial c^{(l)}}{\partial z} \quad (4.6)$$

where D_c is the molecular particle diffusion coefficient (set equal to the kinematic viscosity), P_c is a source term and ϵ_c is a sink term. Usually the source and sink terms are zero, except for the computational bed layer in which these terms represent the mass fluxes due to erosion and deposition. The settling velocity (w_s) is assumed positive downwards.

The third term on the right hand side in the transport equation for the turbulent kinetic energy (equation 4.3) represent buoyancy. Erosion (E) and deposition (D) are modelled by the empirical Partheniades-Krone formulation:

$$E = M \left(\frac{\tau_b}{\tau_e} - 1 \right) \quad (4.7)$$

$$D = w_s c_b \left(1 - \frac{\tau_b}{\tau_d} \right) \quad (4.8)$$

where c_b is the near bottom concentration.

4.3 Testcases

Many experiments have been carried out on a two-fluid system consisting of a salt-water layer and a fresh-water layer on top of it. In these experiments turbulence was generated by a shear stress at the free surface and the lower layer was entrained by the turbulent upper layer. The process of entrainment of a lower salt-water layer is well known. For experiments carried out in a wind flume (Kranenburg, 1984), the entrainment rates are reasonably well represented by the expression:

$$\frac{w_e}{u_*} \approx (0.6 \pm 0.1) Ri_*^{-\frac{1}{2}} \quad (4.9)$$

where Ri_* is the overall Richardson number, u_* is the surface-friction velocity related to the wind shear stress and w_e is the the entrainment rate.

Experiments were also carried out on the entrainment of concentrated near-bed layers (Mehta & Srinivas, 1993; Winterwerp *et al.*, 1993; Winterwerp & Kranenburg, 1997a) and it appeared that entrainment of a concentrated near-bed layer resembles the entrainment processes in a fresh/salt water system. Winterwerp & Kranenburg (1997b) derived from their

entrainment model (Kranenburg & Winterwerp, 1997) the following simplified entrainment formula, containing no mud parameters:

$$\frac{w_e}{u_*} = \frac{C_w}{\left[2\lambda\frac{H}{W}\right]^{\frac{1}{2}} (C_q + Ri_*)} \quad (4.10)$$

Where C_w and C_q are model coefficients, λ is the sidewall friction coefficient, H is the thickness of the mixed upper layer and W is the width of the flume. The experiments were carried out in an annular flume in which the flow is driven by a rotating lid. The flume itself rotates in the opposite direction, so as to minimise secondary currents.

When the density difference between the upper and the lower layers is large or the forcing is weak, the lower layer is dragged along by the upper layer due to viscous effects. The result is a decrease in velocity gradients at the interface and therefore a substantially decrease in entrainment rate. This effect has been observed in the two fluid experiments of Winterwerp & Kranenburg (1997a), and the drag of the quiescent concentrated near-bed layer is taken into account in their entrainment model.

4.4 The simulations

The original version of the 1DV POINT MODEL, which implies a constant molecular viscosity of $1 \cdot 10^{-6} \text{ m}^2/\text{s}$, was applied to a two-fluid system consisting of a salt-water layer and a fresh-water layer on top of it, in which turbulence was generated by a shear stress at the free surface. Equations 4.9 and 4.10 provide the opportunity to validate the model for this kind of two-fluid systems. In figure 4.1 the non-dimensionalised entrainment rates are plotted against the overall Richardson number based on the friction velocity (notice the log scales). In this figure two kinds of data are plotted: results with sidewall friction (which can be compared with equation 4.9) and without sidewall friction (which can be compared with equation 4.10).

Simulations were also carried out on the entrainment of a high-concentrated cohesive sediment layer. The only difference in the model between salt and sediment is the fall velocity (the fall velocity of salt-particles is equal to zero). When including a fall velocity of the sediment, the entrainment rates of the sediment differ from the entrainment rate of salt and do not agree with equation 4.10 at all. Equation 4.10 is derived from experiments carried out in an annular flume (Winterwerp & Kranenburg, 1997b). It is concluded that secondary currents were apparent in the annular flume, counterbalancing the fall velocity and reducing the effective fall velocity to zero. Setting the fall velocity equal to zero in the 1DV POINT MODEL resulted in the same entrainment rates as for salt.

From figure 4.1 it can be concluded that simulating initial entrainment rates of a concentrated layer with the standard 1DV POINT MODEL gives reasonable results.

Simulations were also carried out to assess the influence of the high viscosity of the fluid mud layer. The shear rates on top of fluid mud are in the order of 1 s^{-1} , therefore equation 4.1 with $a = 9330$ is being implemented in the mean flow equations of the 1DV POINT MODEL. In case of a constant viscosity the concentrated layer is not dragged along by the overlying layer. This is shown in figure 4.2 where the velocity is zero in the upper part of the concentrated layer. Preliminary results with a variable viscosity (equation 4.1 with $a = 9330$) show that

growth?

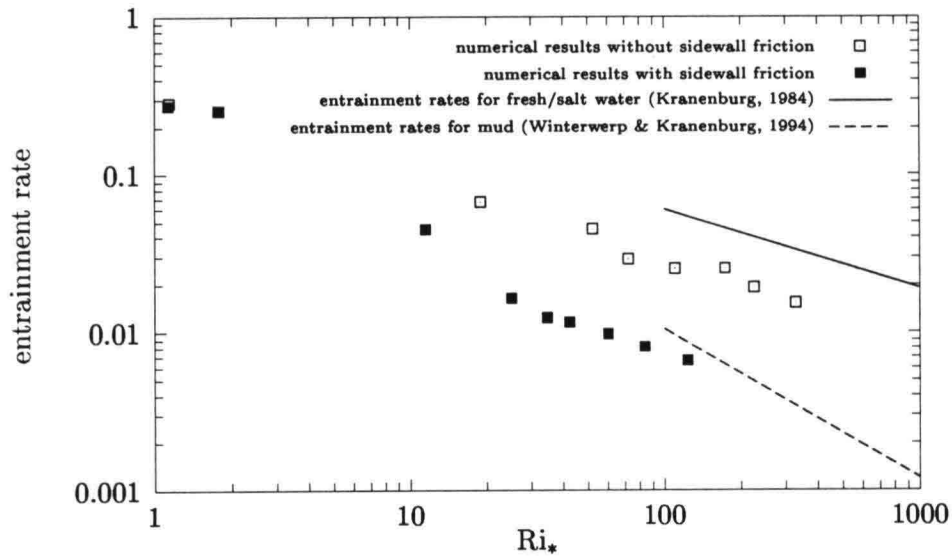


Figure 4.1: Dimensionless entrainment rate $\frac{W_a}{u_*}$ versus overall Richardson number Ri_* .

the fluid mud is dragged along by the overlying flowing fluid. This is shown in figure 4.3 where the velocity is not equal to zero in the upper part of the concentrated layer. It is expected that this viscous mean-flow effect reduces the velocity difference across the water-fluid mud interface and results in a decreased resuspension rate. The preliminary results though, do not show a significant decrease in entrainment rates.

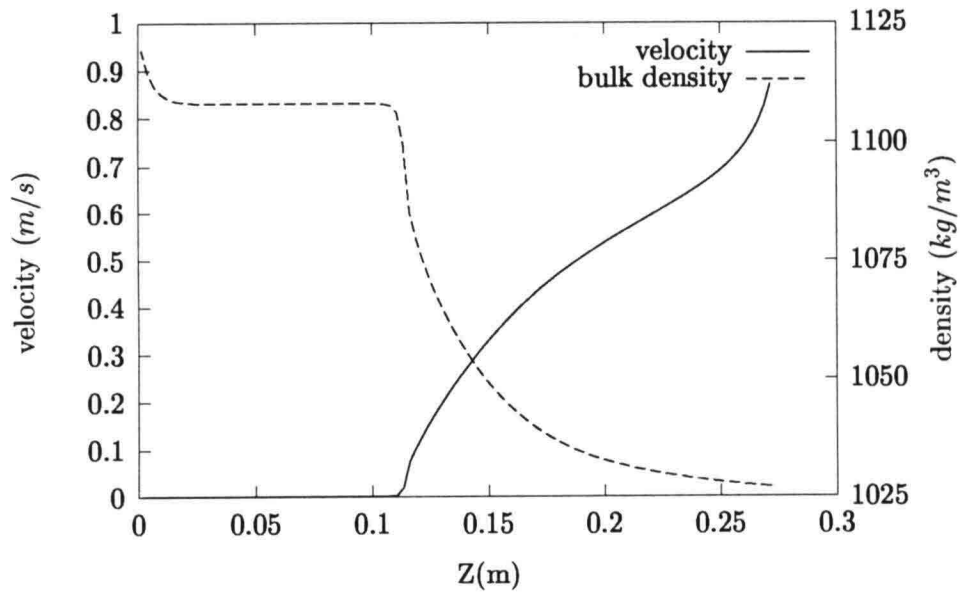


Figure 4.2: Velocity and bulk density profile for a simulation with a constant molecular viscosity.

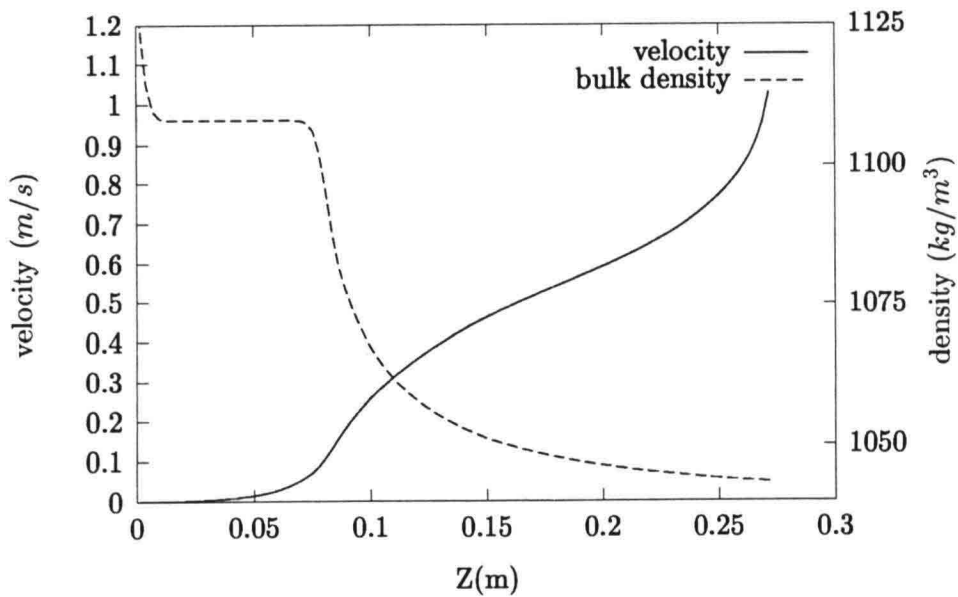


Figure 4.3: Velocity and bulk density profile for a simulation with a variable molecular viscosity, $a = 9330$.

Chapter 5

Future work

5.1 Introduction

The work reported was done in the framework of the COSINUS Project. This project is scheduled to finish in September 2000. This chapter describes the planned near future research activities at Delft University of Technology that links up with the study described in this report.

Subtask A.1 is concerned with sediment induced damping and low Reynolds number flow. Section 5.2 describes the proposed modification of the 1DV POINT MODEL of Delft hydraulics for high Reynolds number flows in order to simulate laminarisation.

Section 5.3 describes a planned laboratory experiment on the entrainment of a dilute suspension by a highly turbulent CBS. This experiment is part of task C.1, laboratory experiments on the dynamics of concentrated benthic suspension layers.

5.2 Modelling laminarisation

One of the objectives of subtask A.1, turbulence modelling of sediment-laden flow, of the COSINUS Project is to extend existing turbulence models in order to simulate sediment-laden flows for a wide range of Reynolds numbers. For situations for which the standard turbulence models do not predict viscous effects which are actually significant (see section 3.3), a low-Reynolds-number turbulence model has to be developed and implemented in the standard turbulence models. Kranenburg (1999) simulated laminarisation of CBS using the Prandtl mixing-length turbulence model supplemented with the Van Driest model of low-Reynolds-number flow.

In collaboration with Delft Hydraulics a low-Reynolds-number adaptation for the 1DV POINT MODEL of Delft Hydraulics (including a $k - \epsilon$ model) is being developed and will be implemented. Laminarisation is a gradual process and therefore it is expected that a $k - \epsilon$ model, including memory effects of turbulence, is a suitable model for simulating this reverse transition.

The first step consists of implementing a damping of the turbulent viscosity at low Reynolds numbers of turbulence in the equations for turbulent kinetic energy, turbulent dissipa-

tion and momentum in the 1DV POINT MODEL:

$$\nu_t = c_\mu f_\mu(Re_t) \frac{k^2}{\epsilon}; \quad Re_t = \frac{k^2}{\nu\epsilon}; \quad f_\mu = 1 - e^{-0.01 Re_t} \quad (5.1)$$

5.3 Annular flume experiments

The objective of the experiments is to study the entrainment process of a dilute suspension by a CBS layer and to obtain data for validation of computer models. The experiments will be carried out in the annular flume of Delft University of Technology in the spring of 1999. In standard annular flumes, the flow is driven by a lid at the water surface and turbulence is generated at this lid, the side walls and possibly at the interface with the bed material (if the material has a certain strength). This configuration is comparable with wind-driven flow in an estuary; the bed material is eroded by a highly turbulent dilute suspension and the bed remains at rest (except for viscous drag). In tidal flow, though, the flow is driven by a pressure gradient. If the bed material is strong enough to resist this pressure gradient, the entrainment process in the standard annular flume is representative for the situation in the field. If, on the other hand, the bed material is not strong enough, the pressure gradient can induce flow in the CBS layer. Turbulence will be generated in this layer, and the dilute suspension will be entrained by this highly turbulent layer (see section 2.3 and 2.4). In order to simulate this entrainment in the annular flume, the driving lid at the water surface is replaced by a bottom plate (Kranenburg & Bruens, 1998). A well mixed suspension is let into the flume and left to rest, so the cohesive sediment is allowed to settle on the bottom plate. Next the speed of the bottom plate is abruptly increased, resulting in a different speed between the bed material and the bottom plate due to inertia of the material. As a consequence of friction between the bottom plate and the bed material turbulence will be generated in this material. The result will be entrainment of water from the overlying layer, a decrease in the density of the lower layer and a rising lutocline, as observed in the field and shown in figure 2.3.

At the time of writing this bottom plate is constructed. Test experiments with fresh and salt water are planned for March 1999. Experiments with an artificial mud (Westwold clay) and a natural mud (from the Caland channel in the Netherlands) are planned to start in April 1999.

Chapter 6

Acknowledgement

This work was carried out as part of the MAST3-COSINUS Project. It was partially funded by the European Commission, Directorate General XII, under Contract No. MAS3-CT97-0082.

I would like to express my gratitude to Dr. C. Kranenburg of the Faculty of Civil Engineering, Delft University of Technology, Mr. H. Winterwerp of WL | delft hydraulics and Dr R. Uittenbogaard also of WL | delft hydraulics, for their many valuable comments and suggestions.

References

- DE WIT, P.J. 1992. *Rheological measurements on artificial muds*. Tech. rept. internal report no. 9-92.
- HIR, P. LE. 1997. Fluid and sediment 'integrated' modelling application to fluid mud flows in estuaries. *In: Cohesive Sediments. 4th Nearshore and Estuarine Cohesive Sediment Transport Conference INTERCOH '94*.
- IVEY, G. N., & IMBERGER, J. 1991. On the nature of turbulence in a stratified fluid. Part I: the energetics of mixing. *Journal of Physical Oceanography*, **21**, 650-658.
- KRANENBURG, C. 1984. Wind-induced entrainment in a stably stratified fluid. *Journal of Fluid Mechanics*, **145**, 253-273.
- KRANENBURG, C. 1998. *In: COSINUS Progress report*.
- KRANENBURG, C. 1999. *Laminarisation in flows of concentrated benthic suspensions. Computations with a low-re mixing-length model*. Tech. rept. 1-99. Delft University of Technology.
- KRANENBURG, C., & BRUENS, A. W. 1998. A flume experiment on CBS dynamics. *In: COSINUS Annual General Meeting, Book of Abstracts*.
- KRANENBURG, C., & WINTERWERP, J.C. 1997. Erosion of fluid mud layers. Part1, Entrainment model. *Journal of Hydraulic engineering*, **123**, 512-519.
- KRONE, R. B. 1962. *Flume studies of the transport of sediment in estuarial shoaling processes*. Tech. rept. Final report, hydr. enrg. and san. enrg. lab. University of California.
- KRONE, R. B. 1986. The significance of aggregate properties to transport processes. *Pages 66-84 of: MEHTA, A. J. (ed), Lecture Notes on Coastal and Estuarine Studies 14 Estuarine Cohesive Sediment Dynamics*. Springer-Verlag.
- LEUSSEN, W. VAN. 1994. *Estuarine macroflocs and their role in fine-grained sediment transport*. Ph.D. thesis, University of Utrecht.
- LIU, K.F., & MEI, C.C. 1990. Approximate equations for the slow spreading of a thin sheet of Bingham plastic fluid. *Phys. Fluids A.*, **2**(1), 30-36.

- MEHTA, A. J., & SRINIVAS, R. 1993. Observations on the entrainment of fluid mud by shear flow. *Coastal and estuarine studies*, **42**, 224–246.
- MEHTA, A.J., & PARTHENIADES, E. 1975. An investigation of the Depositional Properties of Flocculated Fine Sediment. *Journal of Hydraulic Research*, **13**, 361–381.
- MEHTA, A.J., *et al.* 1989. Cohesive Sediment Transport. I: Process Description. *J. Hydr. Eng.*, **115**(8), 1076–1093.
- PARCHURE, T. M., & MEHTA, J. A. 1985. Erosion of soft cohesive sediment deposits. *Journal of Hydraulic Engineering*, **114**-10.
- PARTHENIADES, E. 1962. *A study of erosion and deposition of cohesive soils in salt water*. Ph.D. thesis, University of California.
- PATEL, V. C., RODI, W., & SCHEUERER, G. 1985. Turbulence Models for Near-Wall and Low Reynold Number Flows: A Review. *AIAA Journal*, **23-9**, 1308–1319.
- ROSS, M. A. 1988. *Vertical structure of estuarine fine sediment suspensions*. Ph.D. thesis, University of Florida.
- SILLS, G. G., & ELDER, D. MCG. 1986. The transition from sediment suspension to settling bed. *Pages 192–205 of: MEHTA, A. J. (ed), Lecture Notes on Coastal and Estuarine Studies 14 Estuarine Cohesive Sediment Dynamics*. Springer-Verlag.
- STOLZENBACH, K. D., & RUSSEL, W. B. 1994. The effect of density on collisions between sinking particles: implication for particle aggregation in the ocean. *Journal of Deep Sea Research I*, **41-3**, 469–483.
- TEETER, A. M. 1986. Vertical transport in fine-grained suspension and newly deposited sediment. *Pages 170–191 of: MEHTA, A. J. (ed), Lecture Notes on Coastal and Estuarine Studies 14 Estuarine Cohesive Sediment Dynamics*. Springer-Verlag.
- TEISSON, C. 1997. A review of cohesive sediment transport models. *In: Cohesive Sediments. 4th Nearshore and Estuarine Cohesive Sediment Transport Conference INTERCOH '94*.
- UITTENBOGAARD, R. E. 1995. *The importance of internal waves for mixing in a stratified estuarine tidal flow*. Ph.D. thesis, Delft University of Technolgy.
- UITTENBOGAARD, R. E., WINTERWERP, J. C., VAN KESTER, J. A. T. M., & LEEPEL, H. 1996. *3D cohesive sediment transport; a preparatory study about implementation in DELFT3D*. Tech. rept. z1022. Delft Hydraulics.
- VAN KESSEL, T. 1997. *Generation and transport of subaqueous fluid mud layers*. Ph.D. thesis, Delft University of Technology.
- VAN KESTEREN, W. G. M. 1990. *Orienterende studie baggeren van slib, fase I*. Tech. rept. J493. Delft Hydraulics.

- VAN RIJN, L. 1993. *Transport of Cohesive Materials*. pers. com.
- VERREET, G., & BERLAMONT, J. 1988. *Rheology and non-Newtonian behavior of sea and estuarine mud*. Encyclopedia of Fluid Mechanics, no. VII. Gulf Publications, Houston.
- WAN, Z. 1982. *Bed Material Movement in Hyperconcentrated Flow*. Tech. rept. Series Paper, Lyngby, Technical University of Denmark.
- WINTERWERP, J. C. 1996. *HCBS Hooggeconcentreerde Benthische Suspensie*. Tech. rept. z1013. Delft Hydraulics.
- WINTERWERP, J. C. 1998. *Rapid siltation from saturated mud suspensions*. Tech. rept. intercoh.
- WINTERWERP, J. C. 1999. Ph.D. thesis, Delft University of Technology.
- WINTERWERP, J. C., & KRANENBURG, C. 1997a. Erosion of fluid mud by entrainment. *In: Cohesive Sediments. 4th Nearshore and Estuarine Cohesive Sediment Transport Conference INTERCOH '94*.
- WINTERWERP, J. C., & KRANENBURG, C. 1997b. Erosion of Fluid Mud Layers. II: Experiments and Model Validation. *Journal of Hydraulic engineering*, **123**, 512-519.
- WINTERWERP, J. C., & UITTENBOGAARD, R. E. 1997. *Sediment transport and fluid mud flow; Physical mud properties and parameterisation of vertical transport processes SILTMAN - set-up of a POINT-MUD MODEL*. Tech. rept. z2005. Delft Hydraulics.
- WINTERWERP, J. C., CORNELISSE, J. C., & KUIJPER, C. 1993. A Laboratory Study on the Behavior of Mud from the Western Scheldt under Tidal Conditions. *Coastal and Estuarine Studies*, **42**, 295-313.

List of Figures

1.1	Example of a cross section of a part of an estuary.	3
2.1	The four physical states of a sediment-water mixture.	5
2.2	Diagram of the four classes and the physical exchange processes.	8
2.3	Processes acting in case of a turbulent CBS, (a) a schematic cross section, (b) the density profile showing a rising lutocline, (c) the eddy viscosity profile. . .	13
2.4	Processes acting in case of a turbulent dilute suspension, (a) schematic cross section, (b) the density profile showing a downward moving lutocline, (c) the eddy viscosity profile.	14
2.5	Exchange processes.	14
3.1	Variation of the function f_μ with distance from a smooth wall Patel <i>et al.</i> , 1985. 19	
3.2	The relevance of additional viscous effects for the four different sediment classes. 20	
4.1	Dimensionless entrainment rate $\frac{W_e}{u_*}$ versus overall Richardson number Ri_* . . .	25
4.2	Velocity and bulk density profile for a simulation with a constant molecular viscosity.	26
4.3	Velocity and bulk density profile for a simulation with a variable molecular viscosity, $a = 9330$	26

